Research in Astron. Astrophys. **2012** Vol. **12** No. **1**, 93–103
http://www.raa-journal.org *http://www.iop.org/journals/raa*

***R**esearch in*
***A**stronomy and*
***A**strophysics*

A newly discovered active contact binary in the field of NGC 1348 *

Xiang-Song Fang[1,2,3], Sheng-Hong Gu[1,2], Ho-Keung Hui[4], Chi-Tai Kwok[4], Bill Yeung[5] and Kam-Cheung Leung[5]

[1] National Astronomical Observatories / Yunnan Observatory, Chinese Academy of Sciences, Kunming 650011, China; *xsfang@ynao.ac.cn*
[2] Key Laboratory for the Structure and Evolution of Celestial Objects, Chinese Academy of Sciences, Kunming 650011, China
[3] Graduate University of Chinese Academy of Sciences, Beijing 100049, China
[4] Hokoon Nature Education cum Astronomical Centre, Sik Sik Yuen, Hong Kong, China
[5] Hong Kong Astronomical Society, Hong Kong, China

Received 2011 August 27; accepted 2011 September 15

Abstract We present a CCD photometry study of a newly discovered active eclipsing binary in the field of open cluster NGC 1348 based on the first time-series photometric observation. From the minimum times, we determined an orbital period of $P = 0.691363$ d. Among our datasets, the $BV(RI)_c$ light curves obtained in November 2008 were analyzed using the Wilson-Devinney light curve modeling technique. Because of the uncertainty of the membership of this binary in open cluster NGC 1348, we have analyzed the photometric data in two cases with different primary effective temperatures: Case A ($T_1 = 7750$ K) and Case B ($T_1 = 5250$ K). Our analyses reveal that, for Case A, it is a deep ($f > 70\%$), very low mass ratio ($q \simeq 0.096$) binary system, indicating that it is now in the late evolution stage of a contact binary; while for Case B, it is a red system with extraordinarily long orbital period with respect to the period-color relation for normal contact binaries, which suggests that this binary has evolved off the main sequence. The well known O'Connell effect (e.g., $\Delta B \simeq 0.03$ mag) was found in the dataset obtained in November 2008, which could be due to the existence of starspots on the components, therefore the corresponding spot properties (for Case A: hot spot; for Case B: dark spot) were determined using the Wilson-Devinney code. With the purpose of analyzing the dark spot activity for Case B, we compared the light curves derived in different observing runs, and found that a slight change appeared from November to December, 2008, which indicates the evolution of spot activity on at least one component over a time scale of about one month.

Key words: stars: binaries: close — stars: binaries: eclipsing — stars: spots

∗ Supported by the National Natural Science Foundation of China.

1 INTRODUCTION

In 2008 and 2010 we obtained the first time-series multi-color photometric datasets in the field of NGC 1348 in order to search for variable stars with magnetic activity. NGC 1348 is a poorly studied open cluster, which was identified as Trumpler class III2m (Ann et al. 2002), lying at a distance of about 1900 pc, and has an age greater than 50 Myr (Carraro 2002).

In the field of this open cluster, we discovered a new active EW type eclipsing variable star, GSC2.3 NCB0032066 (= 2MASS J03334546+5125596, hereafter NCB32066), whose finding chart is presented in Figure 1, where the binary is labeled by the symbol "V." In this paper, we derived its orbital period by means of minimum times, and analyzed its light curves with the Wilson-Devinney modeling code (Wilson & Devinney 1971; Wilson 1979, 1990, 1994). In our observations, the light curves in different observing runs changed in the light maximum phases so we also put starspots on the components to find the best solutions. Based on all observed datasets, we studied the light curve variations in different time scales; these variations are often due to starspot activity.

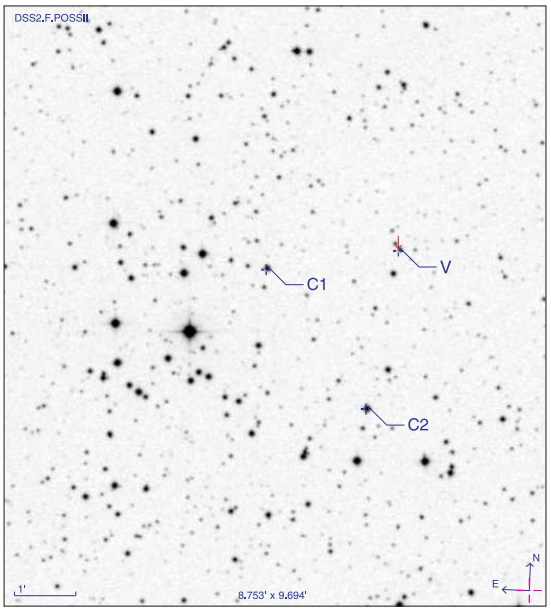

Fig. 1 DSS finding chart in the region of NGC 1348. The binary NCB32066 is marked by the cross with the symbol "V," while the comparison and check stars are labeled "C1" and "C2" respectively.

2 OBSERVATIONS AND DATA REDUCTION

The multi-color photometry in the region of NGC 1348 was performed on five runs in total: 2008 January 18–19, this run was performed using the 1.0 m Cassegrain reflecting telescope equipped with a PI1024 TKB CCD at Yunnan Observatory with RI filters (Yang & Li 1999); 2008 January 10 and 12, November 2-4 and December 1–5, these three runs were carried out using the 85 cm telescope at Xinglong station of NAOC and a 1024×1024/512×512 pixel CCD with standard Johnson-Cousins-Bessell BVRI filters (Zhou et al. 2009); 2010 December 28–30, the fifth run, was performed at Xinglong station on the 80 cm telescope equipped with a Princeton Instrument 1340×1300 pixel CCD and standard Johnson-Cousins VRI filters. The related observing log is shown in Table 1.

Table 1 The Log of Observations for NGC 1348

Date	Bands	Telescope
2008 Jan.10,12	$(RI)_c$	Xinglong 85 cm
2008 Jan.18-19	RI	Kunming 1.0 m
2008 Nov.02-04	$BV(RI)_c$	Xinglong 85 cm
2008 Dec.01-05	$V(RI)_c$	Xinglong 85 cm
2010 Dec.28-30	$V(RI)_c$	Xinglong 80 cm

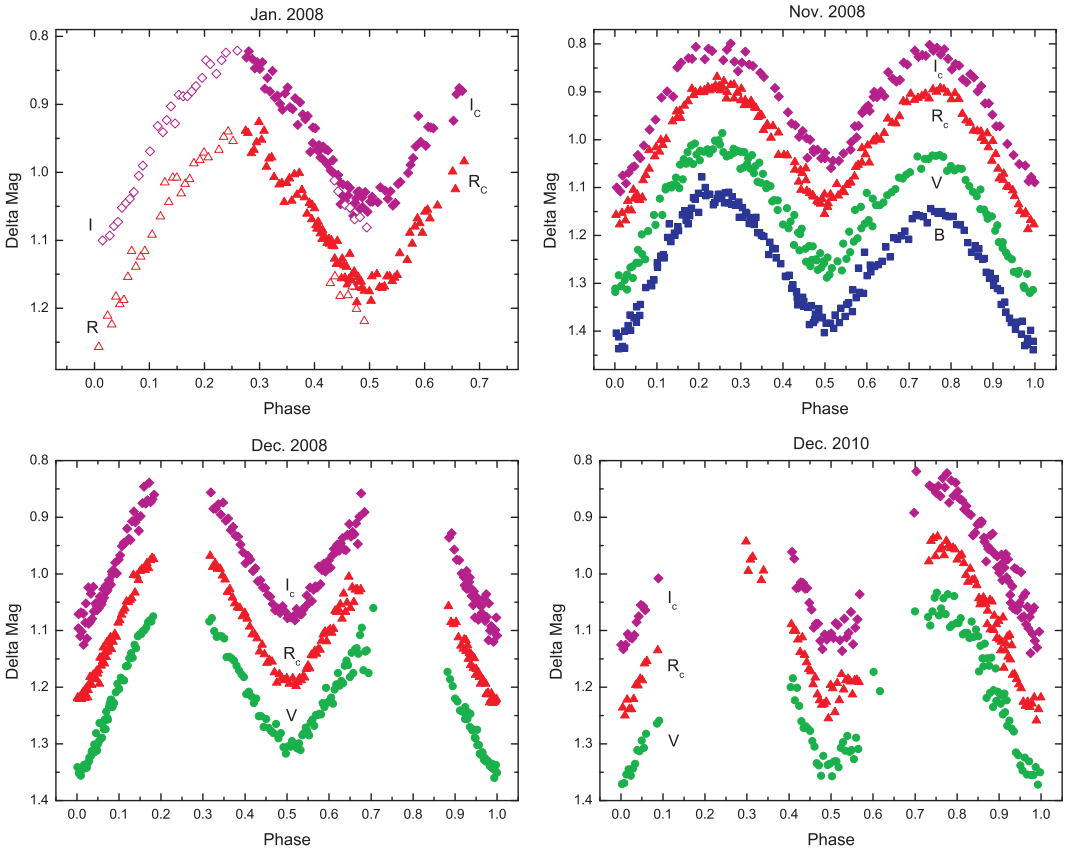

Fig. 2 Multicolor light curves of NCB32066 obtained in 2008 and 2010.

During the data reduction, GSC2.3 NCB0031817 and GSC2.3 NCB0000575 served as comparison and check stars, respectively. Initial reduction of all our raw frames consisted of bias and flat-field corrections, as well as the removal of cosmic ray events. These were performed with the IRAF package in a standard way. The instrumental magnitudes of related stars were obtained by using the PSF fitting method with the IRAF/DAOPHOT package (Stetson 1987) in the slightly crowded field around NCB32066. The standard deviation of the magnitude difference between the comparison and check stars is 0.01 mag more or less for the $BV(RI)_c$ bands in the run of 2008 November 2–4. Unfortunately, the last two runs were plagued by clouds, in particular the observations near the light maximum were obstructed by clouds. The corresponding light curves of this binary in different bands are displayed in Figure 2. Note that the light curves in 2010 December have large observational dispersions due to poor weather conditions during the run.

Table 2 Times of Minima of NCB32066 Obtained in 2008

HJD	Error	E	$O-C$	Label
2454476.04043	0.00110	−431.5	0.00026	Y
2454773.32568	0.00167	−1.5	−0.00058	Y
2454774.36778	0.00203	0.0	0.00448	N
2454775.05286	0.00169	1.0	−0.00180	N
2454802.01876	0.00079	40.0	0.00094	Y
2454803.06074	0.00086	41.5	0.00588	N
2454804.09217	0.00101	43.0	0.00026	Y
2454806.16545	0.00056	46.0	−0.00055	Y

Notes: the minimum time labeled by "Y" denotes that it was used to determine the period.

3 PERIOD AND EPHEMERIS

We obtained eight minimum times of NCB32066 based on the photometric observations carried out in 2008, which are listed in Table 2. Each minimum time was the mean of two values determined by two methods, namely, parabola fitting and gauss fitting to the $(RI)_c$ data sets. We calculated the orbital period of NCB32066 with these minimum times using the linear least-squares method. Three minimum times were omitted (labeled by "N" in Table 2), since they deviated too much during the linear fitting, probably due to the contamination of spot activity, as pointed out by Zhang & Gu (2007). The remaining five minima were used to determine the period. Finally, we determined an orbital period of $P = 0.691363$ d for this binary and a linear ephemeris as follows

$$\mathrm{Min.I} = \mathrm{HJD}2454774.3633(\pm0.0003) + 0.691363(\pm0.000002)E. \quad (1)$$

In Figure 2, the phases correspond to this period.

4 LIGHT CURVE ANALYSIS

4.1 Unspotted Modelings

We solved the $BV(RI)_c$ light curves obtained in the run 2008 November 2–4 with the 2003 version of the Wilson-Devinney modeling code (Wilson & Van Hamme 2004), since this dataset had a full coverage of phase. Before modeling the light curves, the initial values of several basic parameters should be specified, such as the effective temperature of the primary.

Carraro (2002) studied the membership of stars in the region of NGC 1348 and isolated only 20 members, but unfortunately did not give the membership information about NCB32066. Therefore, we derived its primary temperature in two cases based on whether it is a member of NGC 1348, as follows.

Case A: If NCB32066 is one member of the open cluster NGC1348, it thus has color $(B-V)_0 = 0.19 - 0.36$, based on $(B-V) = 1.2098 \pm 0.0489$ of NCB32066 (Carraro 2002), as well as the reddening $E(B-V) = 1.02 \pm 0.05$ (Ann et al. 2002) and $E(B-V) = 0.85 \pm 0.15$ (Carraro 2002) for NGC 1348. In addition, we obtained $(R_c - I_c) = 0.72$ from the dataset of 2008-01-12 using the color transformation of the 85 cm telescope (Zhou et al. 2009), which corresponds to a real color $(R_c - I_c)_0 = 0.09$ (approximately corresponding to a value of $(B-V)_0 = 0.15$), taking into account $E(R_c - I_c) = 0.74E(B-V)$ (He et al. 1995). These above color indices indicate a spectral type of late A or early F for this binary system.

Case B: If the binary is not a member of NGC 1348, e.g., it is a field star in front of NGC 1348, we do not know the influence interstellar reddening has on it. We estimated its effective temperature based on the 2MASS J and H magnitudes using the following relation obtained by Collier Cameron et al. (2007)

$$T_{\rm eff} = -4369.5(J-H) + 7188.2, \qquad 4\,000\,\mathrm{K} < T_{\rm eff} < 7\,000\,\mathrm{K}, \quad (2)$$

considering that the infrared photometry is less reddened than those in B and V bands. The above relation together with $J = 13.736 \pm 0.032$ mag and $H = 13.307 \pm 0.033$ mag (Cutri et al. 2003) gave $T_{\rm eff} = 5314 \pm 200$ K, suggesting it is a late G spectral type binary.

On the other hand, we also estimated its temperature using the interstellar reddening-free quantity (Johnson & Morgan 1955; Hovhannessian 2004)

$$Q = (U-B) - (E_{U-B}/E_{B-V})(B-V) = (U-B)_0 - (E_{U-B}/E_{B-V})(B-V)_0\,, \quad (3)$$

where E_{U-B}/E_{B-V} is the ratio of the corresponding color excesses, which have different values for stars of various spectral types. Straizys et al. (1976) studied this ratio in detail for a normal interstellar reddening law, and found that this ratio varies as a function of $(B-V)_0$ (see table 3 and fig. 4 in their paper). We thus obtained the relationship of Q and $(B-V)_0$ by an interpolation method based on $(U-B)_0$ and $(B-V)_0$ values from Cox (2000). Generally, there are several values of $(B-V)_0$ corresponding to each Q value. Based on the photometric data of NGC 1348 performed by Carraro (2002), who obtained $(U-B) = 0.8473 \pm 0.0688$ mag and $(B-V) = 1.2098 \pm 0.0489$ mag for NCB32066, and Equation (3), we calculated several Q values corresponding to different initial values of E_{U-B}/E_{B-V} (hence $(B-V)_0$). However, as mentioned above, there may be several values of $(B-V)_0$ which correspond to each calculated Q, therefore, comparing these resulting values for each Q with the value $(B-V)_0$ derived from the initial value of E_{U-B}/E_{B-V}, based on the relation of E_{U-B}/E_{B-V} versus $(B-V)_0$, we obtained two self-consistent values corresponding to Case A and Case B, respectively, namely $(B-V)_0 \simeq 0.2$ and $(B-V)_0 \simeq 0.8$ (e.g. 7890 K and 5170 K, according to Cox 2000). Finally, based on the different results mentioned above, we took the values $T_{\rm eff} = 7750$ K and $T_{\rm eff} = 5250$ K as the effective temperature of the primary component of NCB32066 for Case A and Case B, respectively.

The fixed parameters in the modeling procedure were set as follows: temperature of primary T_1, the bolometric albedos $A_{1,2}$, the gravity darkening coefficients $g_{1,2}$ and the linear limb darkening coefficients (from tables of Claret 2000). For Case A, $T_1 = 7750$ K, $A_1 = A_2 = 1.0$, $g_1 = g_2 = 1.0$; for Case B, $T_1 = 5250$ K, $A_1 = A_2 = 0.5$ (Ruciński 1969), $g_1 = g_2 = 0.32$ (Lucy 1967). The adjustable parameters were as follows: inclination i, temperature of the secondary T_2, relative luminosity of the primary L_1, and dimensionless surface potentials $\Omega_{1,2}$.

The up to date spectroscopically determined mass ratio of NCB32066 is not known, therefore we fixed the mass ratio at different values between 0.1–10 in the modeling procedure with a usual q-search method (e.g. Li et al. 2001). For each fixed q, the modeling run started from mode 2 (for detached binaries). For Case A, the solutions corresponding to some cases of fixed q could converge to both mode 3 (appropriate for contact binaries, the components of which are in geometrical contact but not in thermal contact, see Wilson 1979) and mode 4 (semidetached mode with a lobe filling primary). However, the residual $\sum \omega_i (O-C)_i^2$ corresponding to mode 4 was much larger than that of mode 3; we therefore adopted the mode 3 for Case A. For Case B, we found that the solution converged well with mode 3. We found that the minimum residual was achieved for these at $q = 0.15$ and $q = 0.29$ for Case A and Case B, respectively (see Fig. 3). Therefore, we performed the modeling procedures with the adjustable mass ratio having the initial value $q = 0.20$ (for Case A, in practice, it was very hard to get a converged solution with the initial value $q = 0.15$, but it rapidly converged for $q = 0.20$) and $q = 0.29$ (for Case B) to search for the final solutions. The corresponding parameter sets which were finally adopted are listed in the fourth column of Table 3 and Table 4 for Case A and Case B, respectively.

4.2 Spot Fittings

From the light curves obtained in 2008 November, especially the B band light curve, we found that there were differences between the light maxima (e.g., $\Delta B \simeq 0.03$ mag), which is known as the O'Connell effect (O'Connell 1951). Such an effect can be commonly explained by several starspots

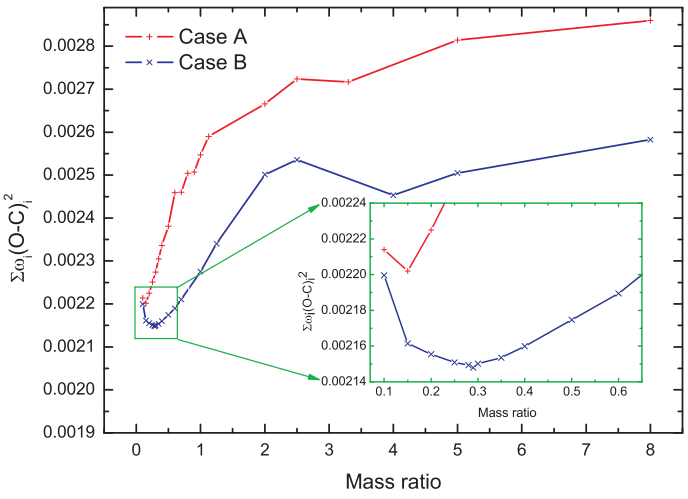

Fig. 3 Residuals of solutions vs mass ratio for both cases.

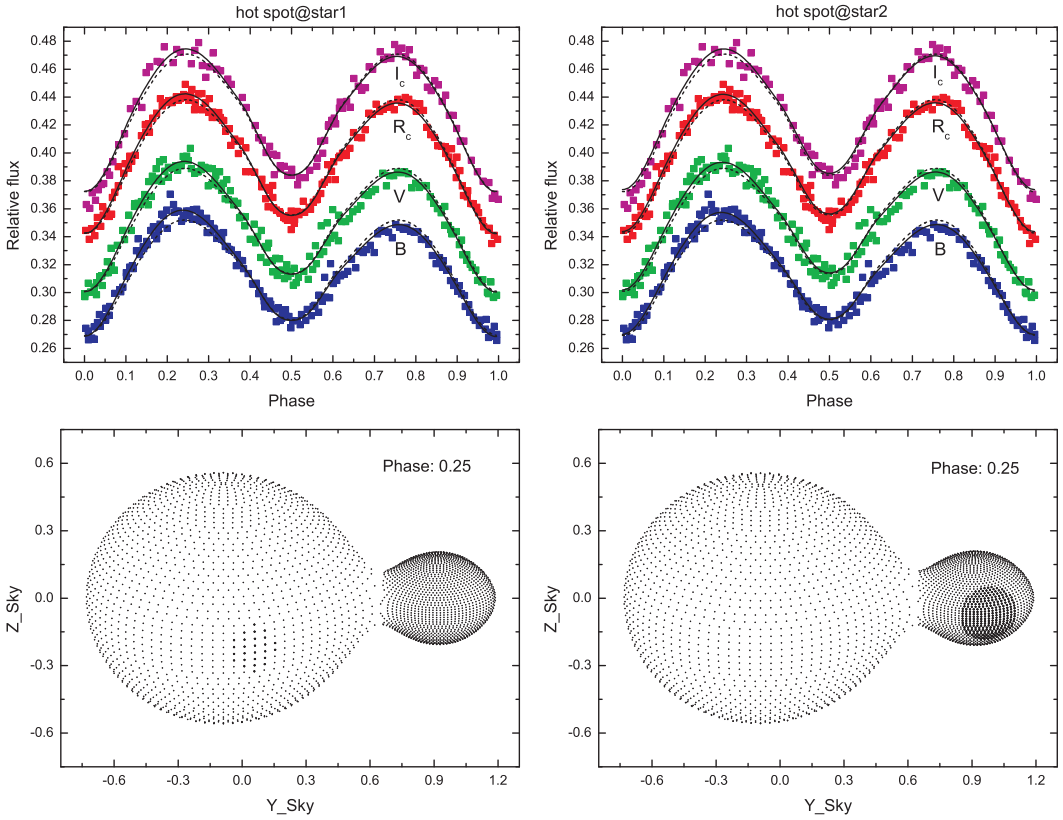

Fig. 4 *Top*: plots of the theoretical light curves with observed data superimposed (Case A), where the filled squares denote the observed data points, and the solid lines and dashed lines refer to the theoretical solutions with spotted and unspotted fittings respectively. *Bottom*: locations of spots on the components.

Table 3 Photometric Solutions of NCB32066 (Case A)

Elements	Case A1(spot@star1)	Case A2(spot@star2)	Unspotted Solution
T_1	7750 K	7750 K	7750 K
A_1=A_2	1.00	1.00	1.00
g_1=g_2	1.00	1.00	1.00
T_2	7005 ± 54 K	7003 ± 59 K	7107 ± 68 K
i	$67.886^\circ \pm 0.998^\circ$	$66.400^\circ \pm 1.168^\circ$	$67.840^\circ \pm 1.253^\circ$
Ω_1=Ω_2	1.9021 ± 0.0159	1.9137 ± 0.0218	1.8902 ± 0.0021
$q = M_2/M_1$	0.096 ± 0.004	0.101 ± 0.007	0.093 ± 0.002
$(L_1/(L_1+L_2))_B$	0.9244 ± 0.0008	0.9215 ± 0.0012	0.9190 ± 0.0010
$(L_1/(L_1+L_2))_V$	0.9153 ± 0.0008	0.9120 ± 0.0012	0.9112 ± 0.0009
$(L_1/(L_1+L_2))_{R_c}$	0.9092 ± 0.0007	0.9056 ± 0.0012	0.9061 ± 0.0009
$(L_1/(L_1+L_2))_{I_c}$	0.9031 ± 0.0007	0.8993 ± 0.0011	0.9009 ± 0.0008
$f(\%)$	70.9	73.6	77.2
$\mathrm{Latitude_{spot}}$	0.0°	0.0°	
$\mathrm{Longitude_{spot}}$	$283.2^\circ \pm 4.2^\circ$	$108.0^\circ \pm 6.6^\circ$	
$\mathrm{Radius_{spot}}$	$10.8^\circ \pm 1.1^\circ$	$36.1^\circ \pm 1.8^\circ$	
$f_\mathrm{s} = T_\mathrm{s}/T_\mathrm{ph}$	1.171 ± 0.010	1.124 ± 0.007	
$\omega_i(O-C)_i^2$	0.001654	0.001735	0.002278

Notes: T_1, A_1=A_2, g_1=g_2 and $\mathrm{Latitude_{spot}}$ were fixed in the modeling runs.

Table 4 Photometric Solutions of NCB32066 (Case B)

Elements	Case B1(spot@star1)	Case B2(spot@star2)	Unspotted Solution
T_1	5250 K	5250 K	5250 K
A_1=A_2	0.50	0.50	0.50
g_1=g_2	0.32	0.32	0.32
T_2	4935 ± 20 K	4952 ± 21 K	4927 ± 23 K
i	$61.470^\circ \pm 0.337^\circ$	$61.186^\circ \pm 0.349^\circ$	$61.203^\circ \pm 0.397^\circ$
Ω_1=Ω_2	2.3826 ± 0.0207	2.3991 ± 0.0213	2.3895 ± 0.0233
$q = M_2/M_1$	0.286 ± 0.008	0.294 ± 0.009	0.290 ± 0.010
$(L_1/(L_1+L_2))_B$	0.8228 ± 0.0012	0.8156 ± 0.0013	0.8227 ± 0.0014
$(L_1/(L_1+L_2))_V$	0.8072 ± 0.0012	0.8004 ± 0.0013	0.8067 ± 0.0014
$(L_1/(L_1+L_2))_{R_c}$	0.7991 ± 0.0012	0.7925 ± 0.0013	0.7983 ± 0.0014
$(L_1/(L_1+L_2))_{I_c}$	0.7930 ± 0.0012	0.7867 ± 0.0013	0.7920 ± 0.0014
$f(\%)$	29.3	29.3	30.1
$\mathrm{Latitude_{spot}}$	45.0°	45.0°	
$\mathrm{Longitude_{spot}}$	$89.9^\circ \pm 2.5^\circ$	$265.0^\circ \pm 15.7^\circ$	
$\mathrm{Radius_{spot}}$	$8.7^\circ \pm 0.2^\circ$	$13.8^\circ \pm 3.6^\circ$	
$f_\mathrm{s} = T_\mathrm{s}/T_\mathrm{ph}$	0.75	0.75	
$\omega_i(O-C)_i^2$	0.001648	0.001750	0.002148

Notes: T_1, A_1=A_2, g_1=g_2, $\mathrm{Latitude_{spot}}$ and f_s were fixed in the modeling runs.

with lower or higher temperature than that of an unspotted photosphere. Here we introduce a spot to reconstruct this effect. For Case B, considering the lower temperature of NCB32066, we introduced a dark starspot to generate the observed O'Connell effect; while for Case A, we explained that by a hot spot instead.

Unfortunately, there are degeneracies in the solution of spot parameters from light curves (Hrivnak et al. 1995; Eker 1996; Eker 1999), e.g., the radius of the spot strongly correlates with its temperature in the fitting run. To ameliorate this, for Case B, we kept the temperature factor $f_\mathrm{s} = T_\mathrm{s}/T_\mathrm{ph}$ (the ratio of the spot's temperature to that of the unspotted photosphere) fixed at a value of 0.75 during the fitting runs, we chose the spot to be located at an intermediate latitude 45°, and we arbitrarily placed a circular dark spot on the primary and secondary (Case B1: one dark

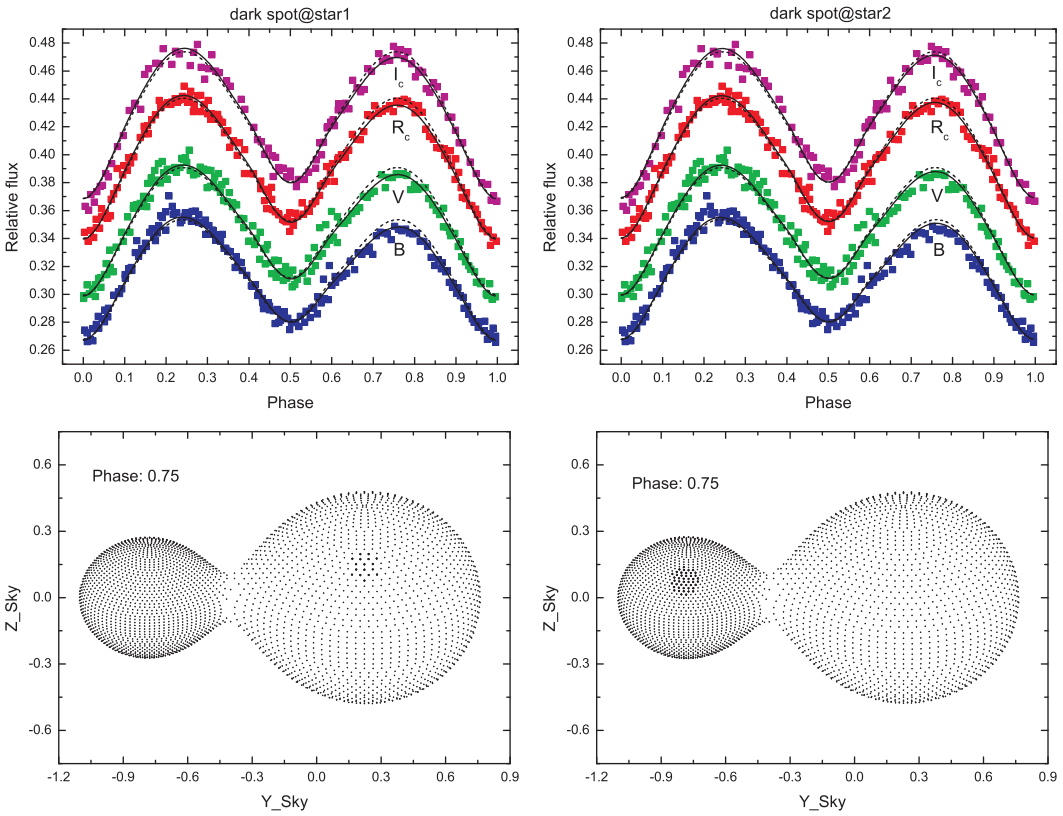

Fig. 5 Same as Fig. 4 but for the case of the primary having a lower temperature of 5250 K (Case B).

spot on the primary, Case B2: one dark spot on the secondary). In the spot fitting runs for this case, the spot parameters (longitude and radius) were adjusted while other parameters were fixed and vice versa; we continued this iteration until convergence. For Case A, we chose a circular hot spot ($f_{\rm s} > 1.0$) to be located at the equator on the primary (Case A1) or secondary (Case A2), considering that the hot spot usually results from heating due to mass transfer between the components through the neck of the Roche lobe. The difference with Case B is that the temperature factor was adjustable, and adjusting this factor was not synchronous with adjusting the longitude and radius of the hot spot in the spot fitting runs. The results are listed in Table 3 (Case A) and Table 4 (Case B); correspondingly, Figure 4 (Case A) and Figure 5 (Case B) show the plots of the theoretical light curves (both unspotted and spotted modelings) with the observed data points superimposed. The corresponding locations of the spots on the components are also shown in the figures.

5 DISCUSSION AND CONCLUSIONS

The solutions we derived show that this binary is a contact binary system for both cases, as expected by the shape of the light curves. We have noticed that, as shown by Kähler (2002) from the work of Eggen (1967), there is a so-called period-color relation for contact binaries

$$1.5 \log T_{\rm eff} - \log P = 5.975 \ldots 6.15, \tag{4}$$

which indicates the temperature of NCB32066 should be in the range from 7500 to 9800 K, approximately, based on its orbital period. We also noticed the work of Kreiner et al. (2006), who derived a new formula describing the period-color relation based on a more numerous and homogeneous statistical analysis than before as follows

$$(B-V)_{\rm cal} = 0.363 + 0.362\log P + 1.99(\log P)^2, \quad (5)$$

which results in a color $(B-V) = 0.356$ for NCB32066 based on its period. One can see that, for Case A, the temperature of NCB32066 is more or less in agreement with this period-color relation; while for Case B, the color is much redder than other known contact binaries with similar period. In other words, the period $P = 0.691363$ d is extraordinarily long for a contact binary with a temperature of about 5250 K. However, we cannot think Case B is unreasonable only based on this big deviation from the period-color relation. In fact, there exist similar binaries whose colors have a large discrepancy from that predicted by the period-color relation. One example is V371 Cep, which is a red evolved binary with a $B-V$ color of more than 0.8 and a period of 0.586 d (Kaluzny & Shara 1987; Rucinski 1994), and in particular, showing some variability in the shape of light curves during the observing run from 2002 Sep. 9 to 2003 Dec. 17 (Mochejska et al. 2008) and is an X-ray source (Gondoin 2005). Similar to V371 Cep, maybe NCB32066 has evolved off the main sequence with a larger volume and hence has a longer orbital period than normal contact binaries, since in this case a larger radial separation can satisfy a contact configuration with a longer period. On the other hand, the long period may partly arise from the mass transfer in the common envelope, since mass transfer can mix the surface abundance (Rubenstein 2001) and hence expand the structure of the star due to increasing the opacity of metal coming from the interior of the star.

For Case A, one can find that it has a very small mass ratio, namely $q \approx 0.093 - 0.101$, approaching the minimum mass ratio of W UMa-type binary systems (Arbutina 2007, 2009). In addition, the filling factor is very large ($f > 70\%$), indicating that it is a deep, very low mass ratio binary. There are several binaries with very low mass ratio and deep contact degree, for example, V857 Her ($q = 0.065$, Qian et al. 2005), V870 Ara ($q = 0.082$, Szalai et al. 2007), FP Boo ($q = 0.096$, Gazeas et al. 2006) and so on. These belong to an interesting class of binaries which are thought to be progenitors of FK Com type stars or blue stragglers (Qian et al. 2006; Arbutina 2009). In fact, one can imagine that, as the binary loses its angular momentum through the magnetized stellar wind or some other process, the radial separation between the components of the binary will decrease, which will result in the shrinking of Roche lobe size, thus the filling factor will increase until it converges into a single, rapidly rotating star, e.g. an FK Com type star or a blue straggler, as mentioned above.

We observed an O'Connell effect on 2008 November 2–4, with $\Delta B \simeq 0.03$ mag. We explained it by starspots for both cases here and thus put starspots on the components to get the best solutions: for Case A, only one bright spot was located on the primary or secondary component, while for Case B, a dark spot was introduced into the primary or secondary of the binary. From Table 3 and Table 4, one can find that the residuals in Case 1 (Case A1 and Case B1) are lower than those in the rest of Case A/B, which indicates that the solutions in Case 1 are more reasonable, in other words, the starspot might be located on the primary component in both cases.

Here we only focus on Case B, where the dark spot commonly correlates with magnetic activity on the components of the binary. In order to analyze the evolution of spot activity, we compared the light curves obtained in different observing runs, as shown in Figure 6. From Figure 6, one can find that there existed a slight change from November 2008 to December 2008 near the phase 0.5–0.7, which indicates that the spot activity evolved over the time scale of about one month. However, we cannot find any change from 2008 to 2010, partly owing to large noise in the dataset of 2010 December.

Although there is uncertainty in the membership of NCB32066 in open cluster NGC 1348, we have resolved the photometric light curves in two cases: Case A with effective temperature of primary $T_1 = 7750$ K and Case B with $T_1 = 5250$ K. Our solutions, based on photometric data

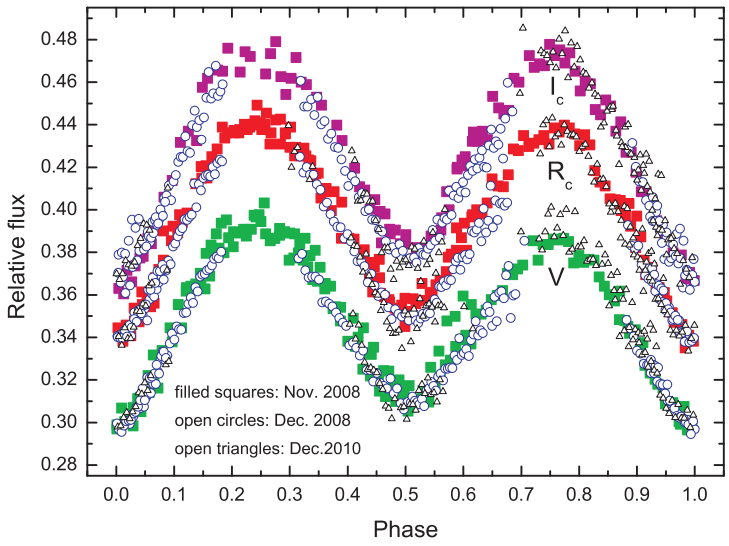

Fig. 6 Multicolor light curves of NCB32066 obtained in 2008 and 2010. Note that the data obtained in different observing runs were shifted vertically to make them have the same values at the phase 0.0.

obtained in Nov. 2008, show that NCB32066 is an interesting object, for both Case A and Case B. In Case A, it is a deep, very low mass ratio contact binary system, indicating that it is now in the late evolution stage of a contact binary; for Case B, it is a red system with an extraordinarily long orbital period compared to other normal contact binaries, sharply deviating from the so-called period-color relation, which suggests that this binary has evolved off the main sequence. Unfortunately, just based on current data, we cannot confirm which is the real case; further observations are indeed needed for this binary system.

Acknowledgements We would like to thank the observing assistants of the 1.0 m telescope at Yunnan Observatory and the 80 cm and 85 cm telescopes at Xinglong station for their support during our observing runs. This work is supported by the National Natural Science Foundation of China (Grant Nos. 10373023 and 10773027) and grants from the Sik Sik Yuen of Hong Kong, China.

References

Ann, H. B., Lee, S. H., Sung, H., et al. 2002, AJ, 123, 905
Arbutina, B. 2007, MNRAS, 377, 1635
Arbutina, B. 2009, PASP, 121, 1036
Carraro, G. 2002, A&A, 387, 479
Claret, A. 2000, A&A, 363, 1081
Collier Cameron, A., Wilson, D. M., West, R. G., et al. 2007, MNRAS, 380, 1230
Cox, A. N. 2000, Allens Astrophysical Quantities 4th ed., (New York: AIP)
Cutri, R. M., Skrutskie, M. F., van Dyk, S., et al. 2003, VizieR Online Data Catalog, 2MASS All Sky Catalog of Point Sources, University of Massachusetts and Infrared Processing and Analysis Center (IPAC/California Institute of Technology)
Eggen, O. J. 1967, MmRAS, 70, 111
Eker, Z. 1996, ApJ, 473, 388
Eker, Z. 1999, ApJ, 512, 386

Gazeas, K. D., Niarchos, P. G., Zola, S., Kreiner, J. M., & Rucinski, S. M. 2006, Acta Astronomica, 56, 127
Gondoin, P. 2005, A&A, 438, 291
He, L., Whittet, D. C. B., Kilkenny, D., & Spencer Jones, J. H. 1995, ApJS, 101, 335
Hovhannessian, R. K. 2004, Astrophysics, 47, 499
Hrivnak, B. J., Guinan, E. F., & Lu, W. 1995, ApJ, 455, 300
Johnson, H. L., & Morgan, W. W. 1955, ApJ, 122, 142
Kähler, H. 2002, A&A, 395, 907
Kaluzny, J., & Shara, M. M. 1987, ApJ, 314, 585
Kreiner, J. M., Zola, S., Ogloza, W., et al. 2006, Ap&SS, 304, 71
Li, L., Liu, Q., Zhang, F., & Han, Z. 2001, AJ, 121, 1091
Lucy, L. B. 1967, ZAp, 65, 89
Mochejska, B. J., Stanek, K. Z., Sasselov, D. D., et al. 2008, Acta Astronomica, 58, 263
O'Connell, D. J. K. 1951, MNRAS, 111, 642
Qian, S., Yang, Y., Zhu, L., He, J., & Yuan, J. 2006, Ap&SS, 304, 25
Qian, S.-B., Zhu, L.-Y., Soonthornthum, B., et al. 2005, AJ, 130, 1206
Rubenstein, E. P. 2001, AJ, 121, 3219
Ruciński, S. M. 1969, Acta Astronomica, 19, 245
Rucinski, S. M. 1994, PASP, 106, 462
Stetson, P. B. 1987, PASP, 99, 191
Straizys, V., Sudzius, J., & Kuriliene, G. 1976, A&A, 50, 413
Szalai, T., Kiss, L. L., Mészáros, S., Vinkó, J., & Csizmadia, S. 2007, A&A, 465, 943
Wilson, R. E. 1979, ApJ, 234, 1054
Wilson, R. E. 1990, ApJ, 356, 613
Wilson, R. E. 1994, PASP, 106, 921
Wilson, R. E., & Devinney, E. J. 1971, ApJ, 166, 605
Wilson, R. E., & Van Hamme, W. 2004, Computing Binary Star Obserables (University of Florida)
Yang, Y., & Li, L. 1999, Publications of the Yunnan Observatory, 1, 32
Zhang, L.-Y., & Gu, S.-H. 2007, A&A, 471, 219
Zhou, A.-Y., Jiang, X.-J., Zhang, Y.-P., & Wei, J.-Y. 2009, RAA (Research in Astronomy and Astrophysics), 9, 349